Adiabatic approach to the dynamics of nonequilibrium electron ensembles in semiconductors

A. A. Grinberg, S. Luryi, N. L. Schryer, and R. K. Smith
AT&T Bell Laboratories, Murray Hill, New Jersey 07974

C. Lee and U. Ravaioli
University of Illinois at Urbana-Champaign, Urbana, Illinois 61801

E. Sangiorgi
University of Udine, Udine, Italy
(Received 15 May 1991)

We describe an approach to the solution of the Boltzmann kinetic equation for the evolution of nonequilibrium electron ensembles in semiconductors under the influence of both phonon scattering and electron-electron interaction. This approach works well when the interaction with optical phonons is the dominant scattering mechanism. In this case, the ensemble evolution can be separated into two stages, the first of which corresponds to the establishment of an intermediate distribution, corresponding to a quasiequilibrium with the optical-phonon subsystem. To describe the subsequent evolution, we assume that this quasiequilibrium is maintained while the ensemble progresses toward the true equilibrium. This assumption implies a certain form of the time-dependent distribution function and renders the full kinetic equation tractable. The solution thus obtained has been checked against Monte Carlo simulations for both polar and nonpolar semiconductors.

I. INTRODUCTION

Description of the time evolution of nonequilibrium electron ensembles is one of the most important problems in applied kinetic theory. Nonequilibrium ensembles arise in a variety of situations: thermionic and tunneling transport in heterojunction barriers, photoexcitation, electron heating by light or electric field, etc. At present, there is no adequate approach to such problems in general—even in the absence of external fields—apart from the reasonably accurate, but computationally slow, Monte Carlo (MC) methods. The purpose of the present work is to propose a computationally efficient semianalytic description of the dynamics of nonstationary electronic ensembles in the absence of an external field and test the validity of this description by MC calculations.

Our approach is physically based on an adiabatic expansion with respect to the small parameter $\tau_{\rm op}/\tau_{\rm in}$, where $1/\tau_{\rm op}$ is a characteristic energy relaxation rate due to the optical-phonon scattering and $1/\tau_{\rm in}$ represents other inelastic-scattering rates. This parameter is indeed small in semiconductors, provided the electron energy is not too high (so that both the intervalley scattering and the impact ionization processes can be neglected) and provided the electron kinetics is not dominated by electron-electron (e-e) scattering. This latter assumption limits the validity of our approach to relatively low ($\lesssim 10^{16}$ cm^{-3}) electron concentrations. An important part of the present work is testing the practical limits on the adiabatic approach posed by the e-e scattering.

The typical problem we consider is as follows: Let $f_i(E)$ be the initial electron-energy distribution at time $t=0$. If f_i is not the equilibrium Boltzmann function, then it evolves in time because of the electron interactions with optical phonons, acoustic phonons, and due to the (e-e) scattering. Under the assumption that $\tau_{\rm op}/\tau_{\rm in} \ll 1$, electrons rapidly establish a quasiequilibrium with the optical-phonon field and then—on a longer scale—the true equilibrium is established by other inelastic-scattering processes. Even though the e-e scattering does not change the average electron energy, it counts as an inelastic interaction for our purposes because, in general, it changes the shape of the nonstationary distribution $f(E,t)$.

For the quasiequilibrium state, the distribution function can be determined from the statistical consideration alone, without actually solving the kinetic equation.[1] This can be done because the optical phonons are to a good approximation monochromatic and therefore do not mix electronic states separated by a noninteger number of optical-phonon energies $\hbar\omega_{\rm op}$. Following Ref. 1, let us divide all electrons into the energy ladders

$$\{E_\nu^{(\varepsilon)}\}=(\varepsilon+\nu)\hbar\omega_{\rm op},\quad 0\le\varepsilon\le 1,\ \nu=0,1,2,\ldots . \tag{1}$$

Here ε is a dimensionless electron energy, defined *modulo* $\hbar\omega_{\rm op}$:

$$\varepsilon=\frac{E\ [\mathrm{mod}(\hbar\omega_{\rm op})]}{\hbar\omega_{\rm op}}\ . \tag{2}$$

By definition, ε is a periodic function of E with a period $\hbar\omega_{\rm op}$; in the first period, $\varepsilon=E/\hbar\omega_{\rm op}$. The total number of electrons on a given ladder will be denoted by $N_{\rm ext}(\varepsilon)$; this number is a functional on the initial distribution $f_i(E)$:

$$N_{\rm ext}[\varepsilon;f_i(E)]=\sum_{\nu=0}^{\infty} D(E_\nu^{(\varepsilon)})f_i(E_\nu^{(\varepsilon)})\ , \tag{3}$$

where $D(E)$ is the electron density of states. The gist of the matter is that $N_{\rm ext}$ is exactly conserved if the interaction with monochromatic optic phonons is the only inelastic-scattering process. The regime where the conservation of $N_{\rm ext}$ is a good approximation will be referred to as *mesoscopic*. In this regime, the distribution function evolves toward a state corresponding to the thermal equilibrium with the optical-phonon subsystem at the lattice temperature T. In that state, characterized by a "mesoscopic equilibrium" distribution $f_m(E)$, the number of electrons on a ladder ε is given by the Gibbs statistics:

$$N_{\rm ext}(\varepsilon,T)=e^{E_F^{(\varepsilon)}/kT}Z(\varepsilon,T)\ , \tag{4}$$

where $E_F^{(\varepsilon)}$ is the chemical potential (Fermi level) of electrons on the ladder ε (note that each ladder has its own $E_F^{(\varepsilon)}$), and Z is the partition function,

$$Z(\varepsilon,T)=\sum_{\nu=0}^{\infty} D(E_\nu^{(\varepsilon)})e^{-E_\nu^{(\varepsilon)}/kT}\ . \tag{5}$$

To the extent that inelastic processes other than optical-phonon scattering can be neglected, i.e., for times

$$\tau_{\rm op}\ll t\ll\tau_{\rm in}\ , \tag{6}$$

all the Fermi levels $E_F^{(\varepsilon)}$ can be obtained from the condition

$$N_{\rm ext}(\varepsilon,T)=N_{\rm ext}[\varepsilon;f_i(E)]\ . \tag{7}$$

Equation (7) determines $E_F^{(\varepsilon)}$ as a function of T and a functional on $f_i(E)$. From this condition, we find that the equilibrium mesoscopic distribution function is given by the following expression:

$$f_m(E)=\exp\left[\frac{E_F^{(\varepsilon)}-E}{kT}\right]=\exp\left[-\frac{E}{kT}\right]\frac{N_{\rm ext}(\varepsilon;f_i)}{Z(\varepsilon,T)}\ . \tag{8}$$

Quite generally, f_m is a periodic function (any function of ε is obviously periodic in E), modulated by the Boltzmann factor. All the above considerations are valid for electronic systems of any dimensionality and an arbitrary energy dispersion relation. For a given analytic form of $f_i(E)$ and assuming a particular model for $D(E)$, we can write f_m down explicitly.

In the parabolic approximation, the density of states of a d-dimensional electronic system is expressed in terms of the effective mass m:

$$D_1(E)=\frac{\sqrt{m}}{\pi\hbar\sqrt{2E}}\ , \tag{9a}$$

$$D_2(E)=\frac{m}{\pi\hbar^2}\ , \tag{9b}$$

$$D_3(E)=\frac{(2m)^{3/2}\sqrt{E}}{2\pi^2\hbar^3}\ , \tag{9c}$$

$$D_d(E)=\frac{2E^{(d-2)/2}}{\Gamma(1+d/2)}\left[\frac{m}{2\pi\hbar^2}\right]^{d/2}\ , \tag{9d}$$

and the partition function (5) can be written in the form

$$Z_d(\varepsilon,T)=\frac{n}{\hbar\omega_{\rm op}}\left[\frac{\hbar\omega_{\rm op}}{kT}\right]^{d/2}\frac{d/2}{\Gamma(1+d/2)}X_\gamma(\varepsilon,\beta)\ ,\qquad \gamma\equiv\frac{d-3}{2} \tag{10}$$

where $\beta\equiv\hbar\omega_{\rm op}/kT$,

$$X_\gamma(\varepsilon,\beta)=\sum_{\nu=0}^{\infty}(\nu+\varepsilon)^{\gamma+1/2}e^{-\beta(\nu+\varepsilon)}\equiv e^{-\beta\varepsilon}\Phi(e^{-\beta},-\gamma-\tfrac{1}{2},\varepsilon)\ , \tag{11}$$

and $\Phi(z,s,v)$ is Weber's function.[2]

For the sake of simplicity, we shall describe the initial nonequilibrium distribution by the Maxwellian ensemble, characterized by a temperature parameter T_i. With the density of states (9d), this corresponds to a distribution function of the form

$$f_i(E)=\frac{nd}{4}\left[\frac{2\pi\hbar^2}{mkT_i}\right]^{d/2}\exp\left[-\frac{E}{kT_i}\right]\ , \tag{12}$$

which is normalized to electron concentration n in units of length^{-d}:

$$\int_0^\infty f(E)D(E)dE=n\ . \tag{13}$$

A narrow initial distribution is modeled by Eq. (12) with $T_i\ll T$ and a broad distribution by $T_i\gg T$. The resultant f_m can be expressed in terms of the ratio of partition functions:

$$f_m(E)=\frac{nd}{4}\left[\frac{2\pi\hbar^2}{mkT_i}\right]^{d/2}\exp\left[-\frac{E}{kT}\right]\frac{Z_d(\varepsilon,T_i)}{Z_d(\varepsilon,T)}\ . \tag{14}$$

For $d=2$, this distribution can be expressed in terms of elementary functions:

$$f_m(E)=\exp\left[-\frac{E}{kT}\right]\exp\left[\varepsilon\hbar\omega_{\rm op}\left[\frac{1}{T}-\frac{1}{T_i}\right]\right]\times\frac{n\pi\hbar^2}{mkT_i}\frac{1-e^{-\hbar\omega_{\rm op}/kT}}{1-e^{-\hbar\omega_{\rm op}/kT_i}}\ . \tag{15}$$

For the three-dimensional case, $d=3$, and for both narrow and broad initial distributions the mesoscopic distribution is shown in Fig. 1. Throughout this work, only the case $d=3$ will be considered.

In the mesoscopic regime, the electronic system possesses a number of unusual thermodynamic and transport properties.[1] For example, the average energy, specific heat, mobility, etc., all behave quite differently than in the true equilibrium. It should be also noted that the mesoscopic regime can be discussed not only in the time domain, but also in spatially nonuniform systems. In this case, the conservation of $N_{\rm ext}$ is expressed by an appropriate continuity equation that involves a vector field called the reduced differential current.[3] These concepts have been proven fruitful in explaining the Hickmott-Eaves oscillations in current-voltage characteristics of heterostrucure tunneling diodes,[4] as well as the energy oscillations in thermionic transport over tri-

angular barriers, discovered recently[5] in MC experiments.

The range expressed by the inequality (6) specifies the mesoscopic regime rather loosely—"for a sufficiently large" disparity between τ_{op} and τ_{in}. An important goal of the present investigation is to concretize the range of validity of the mesoscopic distribution for specific inelastic-scattering mechanisms.

This paper is organized as follows. In Sec. II, we write the kinetic equation in a form convenient for analytic manipulations and describe our model for the collision integral, including terms corresponding to the optical- and acoustic-phonon scatterings and the e-e interaction. Section III describes the initial evolution $f_i \rightarrow f_m$, obtained by solving the kinetic equation with a collision integral that contains the optical-phonon term only. Section IV introduces the adiabatic approximation; it is then used to describe analytically the evolution of f_m toward the true equilibrium under the action of all three inelastic-scattering processes. This evolution can be viewed as the destruction of the mesoscopic order embodied in f_m. Comparison with the results of MC simulations is presented in Sec. V. These simulations have been carried out assuming the parameters of GaAs in the parabolic approximation. The case of nonpolar optical phonons, characteristic of Si or Ge, is also considered, but the e-e scattering is not included in the MC simulation for this case. Our conclusions will be summarized in Sec. VI.

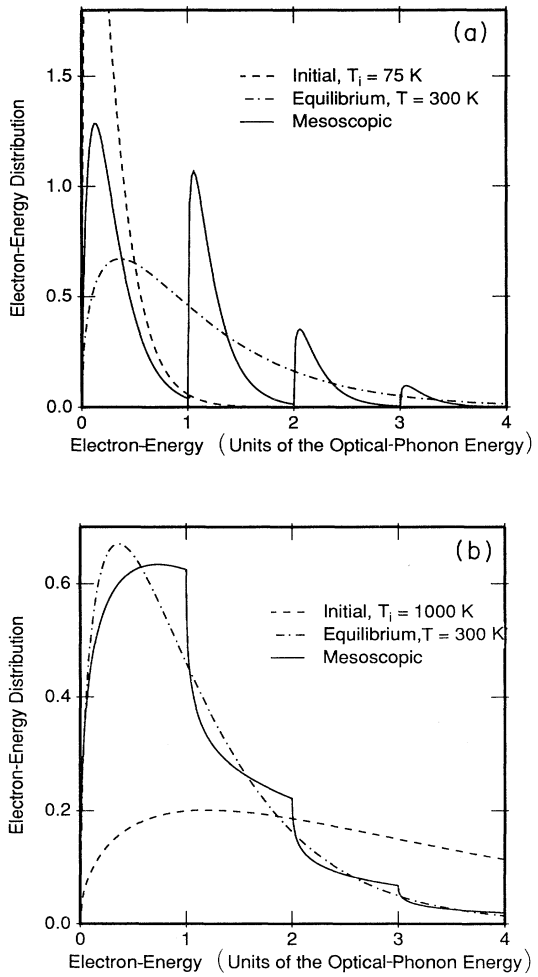

FIG. 1. Electron-energy distributions $(\tilde{E})^{1/2} f_m$ (solid lines) corresponding to the mesoscopic functions $f_m(\tilde{E})$ that evolve from the nonequilibrium Maxwellian ensembles characterized by an initial temperature T_i [Eq. (12)]. The illustrated case corresponds to the lattice temperature $T = 300$ K. The equilibrium distributions are indicated by dash-dotted lines and the initial distributions by dashed lines. (a) $T_i = 75$ K; (b) $T_i = 1000$ K.

II. FORMULATION OF THE TIME-DEPENDENT BOLTZMANN EQUATION

In a spatially uniform system we consider, the electron distribution is spherically symmetric. We shall assume that the electron-energy spectrum is parabolic and isotropic. The kinetic equation, accounting for the optical-phonon, acoustic-phonon, and electron-electron interaction, is of the form

$$\frac{\partial f(E,t)}{\partial t} = \left[\frac{\partial f(E,t)}{\partial t}\right]_{op} + \left[\frac{\partial f(E,t)}{\partial t}\right]_{ac} + \left[\frac{\partial f(E,t)}{\partial T}\right]_{ee}, \tag{16}$$

with the scattering terms given by the following expressions.

Optical phonons:[6]

$$\left[\frac{\partial f(E,t)}{\partial t}\right]_{op} = \frac{1}{\tau_{op}} \frac{4}{(\tilde{E})^{1/2}} \frac{1-e^{\partial/\partial\tilde{E}}}{e^{\beta}-1} \times \{[f(\tilde{E}-1) - e^{\beta} f(\tilde{E})]\chi(\tilde{E})\}, \tag{17}$$

where $\tilde{E} \equiv E/\hbar\omega_{op}$ is a dimensionless electron energy in units of the optical-phonon energy $\hbar\omega_{op}$. The operator $e^{\partial/\partial\tilde{E}}\Psi(\tilde{E}) \equiv \Psi(\tilde{E}+1)$ effects displacements by unity. The function $\chi(\tilde{E})$ and the characteristic time τ_{op} are defined differently for polar and nonpolar optic phonons:

$$\chi(\tilde{E}) = \ln[(\tilde{E}-1)^{1/2} + (\tilde{E})^{1/2}]\Theta(\tilde{E}-1) \quad \text{(polar)}, \tag{18a}$$

$$\chi(\tilde{E}) = [\tilde{E}(\tilde{E}-1)]^{1/2}\Theta(\tilde{E}-1) \quad \text{(nonpolar)}, \tag{18b}$$

$$\frac{1}{\tau_{op}} = \frac{e^2\sqrt{2m\hbar\omega_{op}}}{4\hbar^2}\left[\frac{1}{\epsilon_\infty} - \frac{1}{\epsilon_0}\right] \quad \text{(polar)}, \tag{19a}$$

$$\frac{1}{\tau_{op}} = \frac{E_{op}^2 m^{3/2}(\hbar\omega_{op})^{3/2}}{2^{5/2}\pi\rho s^2\hbar^4} = \frac{(DK)^2 m^{3/2}}{2^{5/2}\pi\rho\hbar^2(\hbar\omega_{op})^{1/2}} \quad \text{(nonpolar)}, \tag{19b}$$

where $\Theta(x)$ is the step function, $E_{op} = (DK)s/\omega_{op}$ is the deformation potential, s is the sound velocity, ρ is the material density, e is the electron charge, and ϵ_∞ and ϵ_0 are, respectively, the optical and the static dielectric permittivities.

Acoustic phonons:[6]

$$\left[\frac{\partial f(\tilde{E},t)}{\partial t}\right]_{ac}=\frac{1}{\tau_{ac}}\frac{1}{(\tilde{E})^{1/2}\beta}\frac{\partial}{\partial\tilde{E}}\times\left[\tilde{E}^2\left[\beta f(\tilde{E})+\frac{\partial f(\tilde{E})}{\partial\tilde{E}}\right]\right], \quad (20)$$

where

$$\frac{1}{\tau_{ac}}=\frac{2^{3/2}E_{ac}^2m^{5/2}\sqrt{\hbar\omega_{op}}}{\pi\rho\hbar^4}, \quad (21)$$

where E_{ac} is the deformation potential for acoustic displacements. Parameters τ_{ac} is the electron-energy relaxation time on acoustic phonons at energies equal to the optical-phonon energy.

Electron-electron interaction:[7]

$$\left[\frac{\partial f(\tilde{E},t)}{\partial t}\right]_{ee}=\frac{1}{(\tilde{E})^{1/2}\tau_{ee}}\frac{\partial}{\partial\tilde{E}}\left\{\ln(1+\alpha\tilde{E}^2)\left[f(\tilde{E})\int_0^{\tilde{E}}(x)^{1/2}f(x)dx+\frac{2}{3}\frac{\partial f(\tilde{E})}{\partial\tilde{E}}\left[\int_0^{\tilde{E}}x^{3/2}f(x)dx+(\tilde{E})^{3/2}\int_{\tilde{E}}^{\infty}f(x)dx\right]\right]\right\}, \quad (22)$$

where

$$\frac{1}{\tau_{ee}}=\frac{2^{1/2}\pi e^4n}{\epsilon_0m^{1/2}(\hbar\omega_{op})^{3/2}}, \quad (23)$$

$$\alpha=\frac{4\epsilon_0L^2(\hbar\omega_{op})^2}{e^4},\quad L=\left[\frac{\epsilon_0\hbar\omega_{op}}{4\pi\beta e^2n}\right]^{1/2}. \quad (24)$$

The *e-e* scattering is nonlinear in the electron concentration n, and hence the concrete form of $(\partial f/\partial t)_{ee}$ depends on the normalization of the distribution function. Since we are interested in the situation when the dominant inelastic interaction is scattering by optical phonons, it is convenient to place the n factor in the scattering rate (23) and normalize the distribution function in terms of the dimensionless energy $\tilde{E}\equiv E/\hbar\omega_{op}$:

$$\int_0^{\infty}f(\tilde{E})\tilde{E}^{1/2}d\tilde{E}=1. \quad (25)$$

In order to convert this function into that with the usual normalization (13) for $d=3$, it must be multiplied by a factor $A_3=3\pi^2\hbar^3n(2m\hbar\omega_{op})^{-3/2}$. With this normalization, the equilibrium function is of the form

$$f(\tilde{E})=\frac{2\beta^{3/2}}{\sqrt{\pi}}e^{-\beta\tilde{E}}. \quad (26)$$

III. INITIAL EVOLUTION TOWARD THE MESOSCOPIC QUASIEQUILIBRIUM

For the distribution f_i of the form (12) with $d=3$, the initial evolution is dominated by optical phonons, even if the carrier is not very low. The reason is that the collision integral (22) vanishes identically for any Maxwellian distribution. Because of that, if we start from this distribution, the *e-e* interaction will be at first inoperative. However, as soon as the initial shape (12) is sufficiently distorted by optical phonons, this is no longer true. Therefore formation of the mesoscopic distribution occurs only if the rate of *e-e* scattering could be neglected compared to that due to optical phonons. This approximation is justified at a sufficiently low electron concentration.

Assuming that this is the case, consider the time evolution solely due to optical phonons. If Eq. (17) represents the only term in the right-hand side of the kinetic equation (16), then the latter can be accurately solved by the following procedure.[1]

First, we note that Eq. (17) does not couple the electron populations belonging to the different ladders (1). Therefore we can split the kinetic equation into a set of independent equations:

$$\frac{\partial\mathbf{f}(\varepsilon,t)}{\partial t}=\hat{\mathbf{M}}(\varepsilon)\mathbf{f}(\varepsilon,t), \quad (27)$$

where we have introduced a multidimensional vector $\mathbf{f}(\varepsilon,t)\equiv\{f_0,f_1,f_2,\ldots\}$ and a matrix $\hat{\mathbf{M}}(\varepsilon)$ with the components

$$f_\nu(\varepsilon,t)\equiv f(\nu+\varepsilon,t),\quad \nu=0,1,2,\ldots \quad (28)$$

$$M_{\nu\mu}(\varepsilon)=\frac{4}{\tau_{op}\sqrt{\varepsilon+\nu}}\frac{1}{e^\beta-1}\times\{\chi(\varepsilon+\nu)\delta_{\nu-1,\mu}-[\chi(\varepsilon+\nu+1)+e^\beta\chi(\varepsilon+\nu)]\delta_{\nu,\mu}+e^\beta\chi(\varepsilon+\nu+1)\delta_{\nu+1,\mu}\}. \quad (29)$$

One of the eigenvalues of $\hat{\mathbf{M}}$ equals zero (this is required for the existence of a stationary solution) and all the other eigenvalues are real and negative. Although formally the matrix is infinite dimensional, in practice it can be truncated without a loss of accuracy. The dimensionality of the truncated matrix is determined by the temperature and the width of the initial distribution relative to $\hbar\omega_{op}$. Truncating the matrix at $\mu,\nu=6$ was adequate for all our examples below. Equation (27) can be efficiently solved by numerically diagonalizing the truncated matrix $\hat{\mathbf{M}}$. The solution,

$$\mathbf{f}(\varepsilon,t)=e^{t\hat{\mathbf{M}}(\varepsilon)}\mathbf{f}_i(\varepsilon), \quad (30)$$

where

$$\mathbf{f}_i(\varepsilon)\equiv\{f_i(\varepsilon),f_i(\varepsilon+1),f_i(\varepsilon+2),\ldots,\}$$

is illustrated in Fig. 2 for polar phonons with $\hbar\omega_{op}=36$ meV, corresponding to the LO phonon in GaAs, $T=300$ K, and two initial distributions of the form (12) with $d=3$. The narrow distribution is specified by $T_i=75$ K and the broad distribution by $T_i=1000$ K. We see that the mesoscopic distribution is largely established by the time of order τ_{op}, which for GaAs equals 0.52 ps.

IV. DESTRUCTION OF THE MESOSCOPIC ORDER BY INELASTIC SCATTERING: ADIABATIC APPROXIMATION

The adiabatic approximation consists in the assumption that as the electron ensemble evolves in time, it stays in equilibrium with the optical phonons. This means that the electron distribution function at any given time is assumed in the form (8), where, however, the periodic part $E_F^{(\varepsilon)}$ is no longer fixed in terms of the initial distribution f_i but varies in time under the action of both the acoustic and the *e-e* scattering processes. Thus the time-dependent function $f(E,t)$ in the adiabatic approximation is given by

$$f(E,t)=\phi(\varepsilon,t)e^{-E/kT}, \tag{31}$$

with the initial condition $f(E,0)=f_m(E)$, or

$$\phi(\varepsilon,0)=\exp\left[\frac{E_f^{(\varepsilon)}}{kT}\right]=\frac{N_{\text{ext}}(\varepsilon;f_i)}{Z(\varepsilon,T)}. \tag{32}$$

The right-hand side of Eq. (17) vanishes for any function of the form (31), i.e., such functions do not evolve under the action of optical phonons alone. Mathematically, this follows from the fact that the term $[f(\tilde{E}-1)-e^{\beta}f(\tilde{E})]$ vanishes. Substituting (31) into Eqs. (20) and (22), multiplying by the density of states $(\tilde{E})^{1/2}$, and summing over the ladder of energies (1), we reduce the kinetic equation (16) into an equation for $\phi(\varepsilon,t)$:

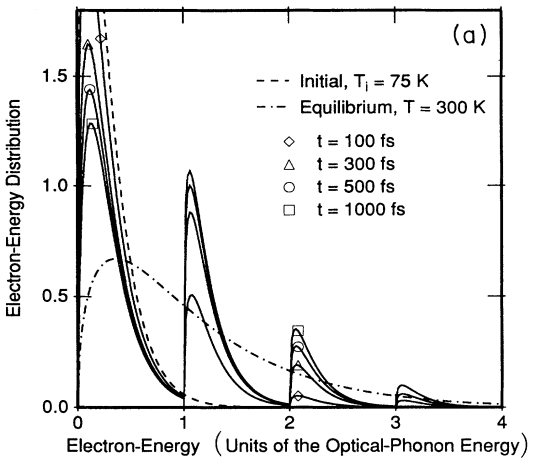

FIG. 2. Time evolution of nonequilibrium Maxwellian ensembles, characterized by an initial temperature T_i, due to the optical-phonon scattering only [Eq. (17)]. The illustrated case corresponds to the lattice temperature $T=300$ K. For $t\gtrsim 2\tau_{op}$ the time-dependent distributions are indistinguishable from the mesoscopic functions $(\tilde{E})^{1/2}f_m(\tilde{E})$ shown in Fig. 1(a). (a) $T_i=75$ K; (b) $T_i=1000$ K.

$$\frac{\partial\phi(\varepsilon,t)}{\partial t}=\frac{1}{X_0(\varepsilon,\beta)}\frac{\partial}{\partial\varepsilon}\left[\frac{1}{\tau_{ee}}\left[\int_0^1 K_1(\varepsilon,\varepsilon')\phi(\varepsilon')d\varepsilon'+\frac{\partial\phi(\varepsilon)}{\partial\varepsilon}\int_0^1 K_1(\varepsilon,\varepsilon')\phi(\varepsilon')d\varepsilon'\right]\right.$$
$$\left.+\frac{1}{\tau_{ac}}\frac{N_\beta}{\beta}\frac{\partial\phi(\varepsilon)}{\partial\varepsilon}e^{-\beta\varepsilon}[\varepsilon^2+2\varepsilon(N_\beta-1)+(N_\beta-1)(2N_\beta-1)]\right], \tag{33}$$

where X_0 is defined by Eq. (11), and

$$N_\beta=(1-e^{-\beta})^{-1}, \tag{34}$$

$$K_1(\varepsilon,\varepsilon')=\sum_{\nu=1}^{\infty}\sum_{\mu=0}^{\nu-1}F_1(\varepsilon+\nu,\varepsilon'+\mu)$$
$$+\Theta(\varepsilon-\varepsilon')\sum_{\nu=0}^{\infty}F_1(\varepsilon+\nu,\varepsilon'+\mu)$$
$$-\beta\sum_{\nu=0}^{\infty}F_3(\varepsilon+\nu,\varepsilon'), \tag{35}$$

$$K_2(\varepsilon,\varepsilon')=\sum_{\nu=1}^{\infty}\sum_{\mu=0}^{\nu-1}F_2(\varepsilon+\nu,\varepsilon'+\mu)$$
$$+\Theta(\varepsilon-\varepsilon')\sum_{\nu=0}^{\infty}F_2(\varepsilon+\nu,\varepsilon'+\mu)$$
$$+\sum_{\nu=0}^{\infty}F_3(\varepsilon+\nu,\varepsilon'), \tag{36}$$

$$F_1(x,y)=[y^{1/2}-\tfrac{2}{3}\beta(y^{3/2}-x^{3/2})]$$
$$\times\ln(1+\alpha x^2)e^{-\beta(x+y)}, \tag{37}$$

$$F_2(x,y)=\tfrac{2}{3}(y^{3/2}-x^{3/2})\ln(1+\alpha x^2)e^{-\beta(x+y)}\ , \quad (38)$$

$$F_3(x,y)=\tfrac{2}{3}N_\beta x^{3/2}\ln(1+\alpha x^2)e^{-\beta(x+y)}\ . \quad (39)$$

It can be shown that $\int_0^1 K_1(\varepsilon,\varepsilon')d\varepsilon'=0$ and, therefore, Eq. (33) is satisfied by $\phi(\varepsilon)=$const.

If the *e-e* interaction is not included, then the evolution of an electron-energy distribution function in the adiabatic approximation is described by a simple differential equation corresponding to the second line in Eq. (33). Its solution is illustrated in Fig. 3 for two initial distributions, described by the mesoscopic functions displayed in Fig. 1. In this calculation, we have used the parameters of GaAs, taking $\tau_{ac}=8.5$ ns, see Table I. We see that approach to the true equilibrium, corresponding to $T=300$ K, occurs over a time of order $0.1\tau_{ac}$. It should be stressed that the parameter τ_{ac} alone does not set the scale for the temporal evolution, because of the strong energy dependence in the right-hand side of (33). As the median electron energy shifts in the course of the evolution, the bottleneck that slows the equilibration occurs when the electron population is weighted heavier toward lower energies.

With the *e-e* interaction included, Eq. (33) represents a rather complicated nonlinear integro-differential equation. It was solved using a general purpose software POST.[8] The solutions were represented in terms of a set of *B*-spline basis functions, as described in the Appendix. For typical runs a total of 25–50 energy points were used resulting in quite modest run times (a few minutes on a Cray Research, Inc. XMP/28 supercomputer for the entire transient solution).

Figures 4(a) and 4(b) illustrate the temporal evolution calculated for the carrier concentration $n=10^{15}$ cm^{-3} in GaAs. The time constant τ_{ee} in this case is about 76 ps, but the approach to equilibrium occurs substantially fas-

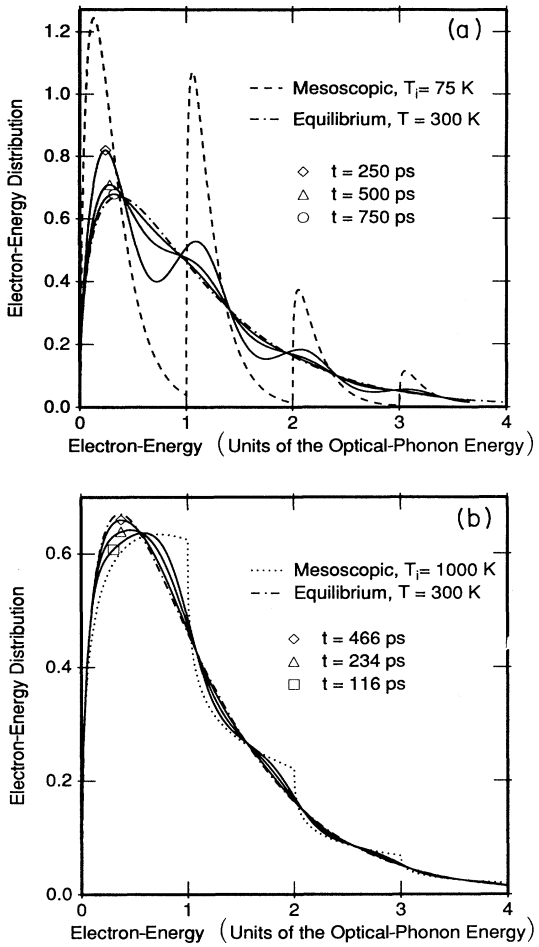

FIG. 3. Evolution of the mesoscopic distributions $(\tilde{E})^{1/2}f_m(\tilde{E})$ under the influence of acoustic phonons in the adiabatic approximation. Lattice temperature $T=300$ K. (a) $T_i=75$ K; (b) $T_i=1000$ K.

TABLE I. Material parameters used.

	Notation	GaAs	Si	Units
Density	ρ	5.36	2.33	g/cm^3
Sound velocity	s	5.24	9.04	10^5 cm/s
Static dielectric constant	ϵ_0	12.9	11.7	
High-frequency dielectric constant	ϵ_∞	10.92		
Optical-phonon energy	$\hbar\omega_{op}$	36	52	meV
Electron effective mass	m	0.067	0.31	m_0
Acoustic deformation potential	E_{ac}	7.0	7.0	eV
Nonpolar optic-phonon coupling constant	DK		1.55×10^9	eV/cm
Characteristic energy relaxation time on optical phonons [Eqs. (19a) and (19b)]	τ_{op}	5.2×10^{-13}	6.9×10^{-13}	s
Characteristic energy relaxation times on acoustic phonons [Eq. (21)]	τ_{ac}	8.5×10^{-9}	6.6×10^{-11}	s
Characteristic (*e-e*) relaxation time at $n=10^{16}$ cm^{-3} [Eq. (23)]	τ_{ee}	7.6×10^{-12}		s

ter. We note again that no single parameter can be used to scale the equilibration rate. In the case of *e-e* scattering this circumstance is due to the nonlinear nature of the equation. In particular, the closer the nonequilibrium distribution to a Maxwellian shape is, the slower is its equilibration under *e-e* interaction.

Examination of the curves in Fig. 4(b), corresponding to the transition from a broad initial distribution, shows a spike at low energies for the short times after $t=\tau_{op}$, i.e., immediately after the adiabatic approximation is turned on. This spike is an artifact of the adiabatic approximation, resulting from the fact that it exaggerates the rate of transitions into the low-energy part of the electron distribution function. In reality, these transitions are suppressed by the low density of states ($\propto\sqrt{E}$ in the three-dimensional case). In the adiabatic approximation, the spike is formed due to the high rate of diffusion in the energy space near the sharp edge of the distribution at $E=\hbar\omega_{op}$ which results in an appreciable population in the region immediately above $\hbar\omega_{op}$ that is "instantly" transferred down by the optical-phonon emission. It remains an open question whether or not such an effect can take place in a realistic scattering model.

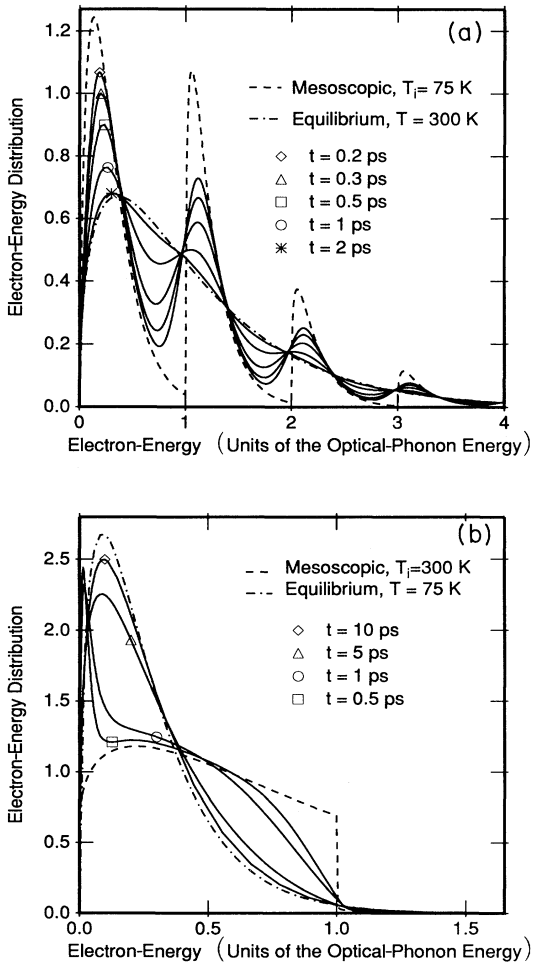

FIG. 4. Evolution of the mesoscopic distributions $(\tilde{E})^{1/2}f_m(\tilde{E})$ under the influence of both acoustic phonons and *e-e* scattering in the adiabatic approximation. Lattice temperature $T=300$ K. Carrier concentration $n=10^{15}$ cm^{-3}. (a) Initial mesoscopic distribution with $T_i=75$ K and $T=300$ K; (b) Initial mesoscopic distribution with $T_i=300$ K and $T=75$ K.

V. NUMERICAL EXAMPLES: COMPARISON WITH MONTE CARLO CALCULATIONS

We have performed a number of numerical simulations with the Monte Carlo codes developed at the University of Illinois[9] and the University of Bologna.[10] The Illinois computer code was used to simulate the temporal evolution of nonequilibrium electron distribution functions in *polar* semiconductors, using the parameters of GaAs and including the *e-e* scattering[11] as well as both optic and acoustic phonons.[12] The Bologna computer code was used to simulate *nonpolar* semiconductors, using the parameters of Si and including phonon scattering only. Parameters assumed in our numerical examples are listed in Table I.

To facilitate the comparison with our analytic results, we assumed parabolic dispersion relations in the MC models used. A comparison with more realistic models showed that this approximation produced no significant loss in accuracy for our examples.

A. Interaction with acoustic phonons only

We begin our comparison by taking an example of Si, including the scattering by phonons only (both optical and acoustic). This example is interesting for two reasons. First, it demonstrates the validity of our approach for nonpolar optical phonons and, second, it illustrates the substantially more rapid degradation of the mesoscopic order by acoustic-phonon scattering (τ_{ac} in Si is more than two orders of magnitude shorter than in GaAs). The distribution functions calculated by MC at several representative times are shown in Fig. 5 by solid lines. Note that, in contrast to Figs. 1–4, we are now plotting the function $f(E)$ itself, without the density-of-states factor $\sqrt{E}$. On a logarithmic scale, therefore, Maxwellian ensembles are represented by straight lines.

The initial distribution is taken as a narrow Maxwellian ensemble, characterized by $T_i=75$ K. As is evident from Fig. 5, the evolution of this ensemble has two distinct regimes. In the first regime, corresponding to times $t\lesssim\tau_{op}$, the mesoscopic order is established by the optical-phonon scattering. In this time range, the MC results agree quite accurately with the analytic solution (30) of Eq. (17). For $t\gtrsim\tau_{op}$, the evolution proceeds in excellent agreement with the adiabatic approximation. To be consistent in the comparison of the MC and the analytic curves at similar times, we have taken the solutions of the adiabatic equation (33) at times shifted by τ_{op}, i.e., for $t\gtrsim\tau_{op}$, we plot $f(E,t-\tau_{op})$ with $f(E,t)$ given by Eq. (31).

We have also performed MC calculations of $f(E,t)$ for polar semiconductors, using GaAs parameters (Table I). In the absence of *e-e* interaction and/or at low carrier

concentrations ($n=10^{14}$ cm^{-3}) the agreement with our analytic results (Figs. 2 and 3) is excellent, quite similar to the case of Si displayed in Fig. 5.

B. Inclusion of the electron-electron scattering and acoustic phonons

Figure 6 shows the MC and the analytic results for GaAs at $n=10^{15}$ cm^{-3}. Both the phonon and the *e-e* scattering mechanisms are included. Evolution from a narrow initial distribution ($T_i=75$ K) to the equilibrium at $T=300$ K is illustrated in Fig. 6(a) and that from a "broad" distribution ($T_i=300$ K to $T=75$ K) in Fig. 6(b).

Already at such low carrier concentration, the evolution of the electron distribution function for $t>\tau_{op}$ is dominated by the *e-e* interaction rather than by acoustic scattering. Indeed, as can be seen from Table I, the characteristic *e-e* scattering time τ_{ee} at $n=10^{15}$ cm^{-3} is of the order 0.8 ps, which is much smaller than τ_{ac}. Agreement with the analytic solution is still quite satisfactory. For the broad initial distribution [Fig. 6(b)], the adiabatic approximation produces an artificial spike at low energies for short times immediately after $t=\tau_{op}$. Although, for certain initial distributions, such a spike may be a real effect, it is certainly exaggerated by the adiabatic approximation, as discussed in connection with Fig. 4(b). No evidence of this effect has been seen in our MC calculations for the examples considered.

Figure 7 illustrates analogous results for $n=10^{16}$ cm^{-3}. We see that the adiabatic approximation still works and the results for $t>\tau_{op}$ are in a reasonable agreement with the MC calculation. However, the evolution prior to τ_{op} is not adequately represented by Eq. (30). The same trend continues at still higher carrier concentrations ($n=10^{17}$ cm^{-3}, not shown). This is as expected, because the validity of Eq. (17) rests on the assumption of the dominant role of optical phonons at short times, an assumption violated by a strong *e-e* interaction. Our results show that the adiabatic approximation works well even at high carrier concentrations, provided the "ini-

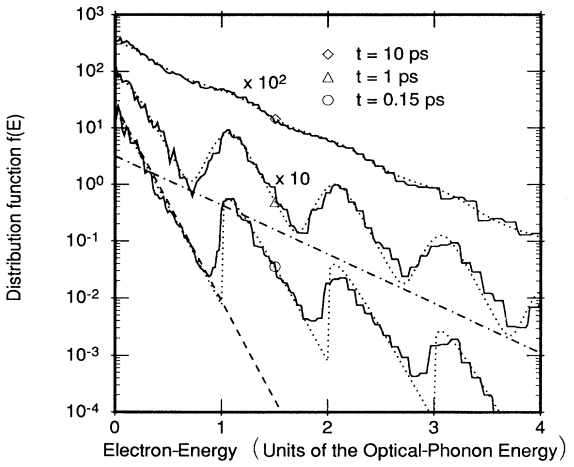

FIG. 5. Monte Carlo simulation of the time development of the distribution function $f(\tilde{E},t)$ (solid lines) subject to scattering by both optic and acoustic phonons at $T=300$ K with the parameters of Si. The initial distribution $f_i(\tilde{E})$ corresponds to a Maxwellian ensemble (12) with $T_i=75$ K (dashed line). The equilibrium distribution is indicated by the dash-dotted line. Dotted lines show the results of analytic calculations: for $t<\tau_{op}$, the solution (30) of Eq. (17); and for $t>\tau_{op}$, the solution of Eq. (33) with $\tau_{ee}=\infty$. For visual convenience, curves corresponding to longer times are shifted with respect to one another by a decade.

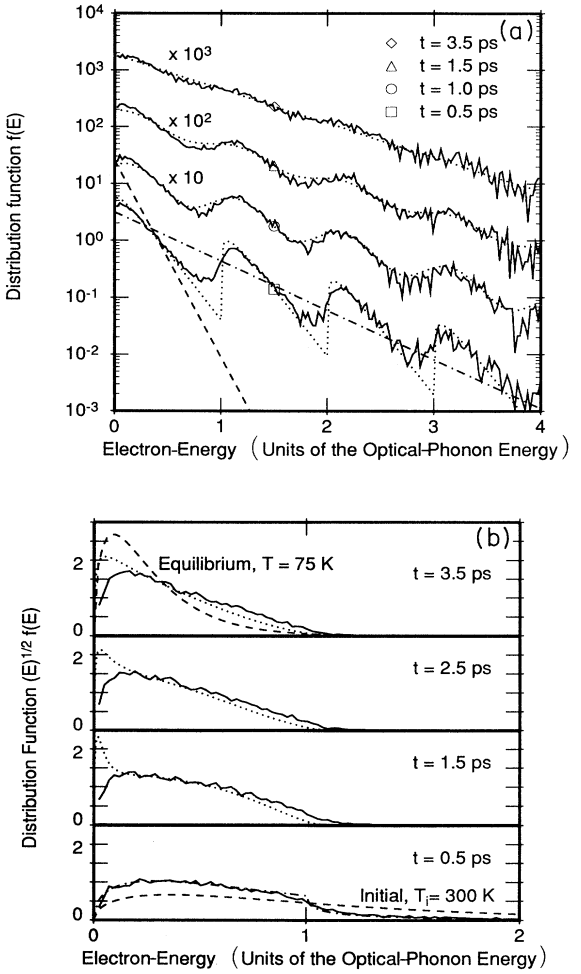

FIG. 6. Monte Carlo simulation of the time development of the distribution function $f(\tilde{E},t)$, including the *e-e* interaction and the scattering by both optic and acoustic phonons. Parameters assumed correspond to GaAs. Carrier concentration $n=10^{15}$ cm^{-3}. The equilibrium and the initial distributions are indicated by the dash-dotted and dashed lines, respectively. Dotted lines show the results of analytic calculations: for $t<\tau_{op}$, the solution (30) of Eq. (17); and for $t>\tau_{op}$, the solution of Eq. (33). For visual convenience, curves corresponding to longer times are shifted in (a) with respect to one another by a decade. In (b), where $(\tilde{E})^{1/2}f(\tilde{E})$ is plotted, the same convenience is achieved by shifting the origin. (a) $T_i=75$ K, $T=300$ K; (b) $T_i=300$ K, $T=75$ K.

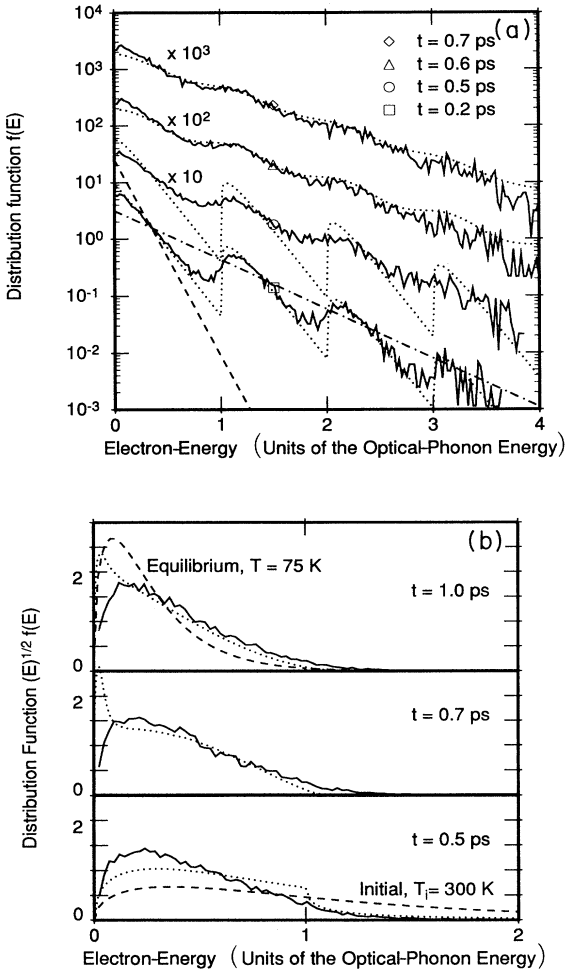

FIG. 7. Same as Fig. 6 but for carrier concentration $n=10^{16}$ cm^{-3}.

tial" distribution at $t=\tau_{op}$ is specified correctly. Moreover, we see that the adiabatic evolution is capable of correcting the mistake introduced by ignoring the *e-e* scattering at $t<\tau_{op}$.

VI. CONCLUSION

We have described an approach to the solution of the Boltzmann kinetic equation for the evolution of nonequilibrium electron ensembles in semiconductors under the influence of both the phonon scattering and the electron-electron interaction. This approach works extremely well when the interaction with optical phonons is the dominant scattering mechanism. In this case, the ensemble evolution can be separated in two stages, the first of which corresponds to the establishment of an intermediate "mesoscopic" distribution, corresponding to a quasiequilibrium with the optical-phonon subsystem. Subsequent evolution is accurately described by what we call the adiabatic approximation, which consists in the assumption that this quasiequilibrium is maintained while the ensemble evolves toward the true equilibrium under the influence of acoustic phonons and the *e-e* scattering. This assumption implies a certain form of the time-dependent distribution function and renders tractable a solution of the full kinetic equation.

The solution thus obtained has been checked against Monte Carlo simulations of both polar and nonpolar semiconductors. We found that adiabatic approximation itself works exceedingly well not only at low carrier concentrations but also in the intermediate-carrier-concentration range (up to $n\sim10^{16}$ cm^{-3}). However, the first stage, corresponding to the establishment of the mesoscopic distribution, becomes progressively less accurate as the *e-e* scattering rate becomes comparable to or exceeds the optical-phonon rate, and already at the electron concentrations of $n\sim10^{16}$ cm^{-3} a significant discrepancy is found. This discrepancy does not indicate the failure of the adiabatic approximation but shows the need for its generalization which would include the *e-e* interaction on equal footing with optical phonons in the initial stage of the evolution. Such a generalization is feasible and will be discussed in a subsequent publication.

ACKNOWLEDGMENT

C.L. and U.R. were supported by the National Science Foundation through the National Center for Computational Electronics of the University of Illinois.

APPENDIX: NUMERICAL SOLUTION OF THE INTEGRAL PDE

The software used to solve Eq. (33) is POST.[8] That software can solve quite general systems of partial differential equations (PDE's), ordinary differential equations (ODE's), and integro-differential equations of the type given by Eq. (33). This appendix describes the general form of equations that can be handled by POST and the formulation of (33) is within that framework.

Let $\mathbf{u}$ be a vector of PDE variables of length n_u and $\mathbf{v}$ be a vector of ODE variables of length n_v. That is, $\mathbf{u}$ depends on space x and time t, while $\mathbf{v}$ depends on time t alone. POST internally represents the solution $\mathbf{u}$ in terms of a set of B-spline[13] basis functions $B_j(x)$, with each component of $\mathbf{u}$ given by

$$u_i(t,x)=\sum_j U_{ji}(t)B_j(x)\ . \tag{A1}$$

Since the B_j are known, all information about $\mathbf{u}(x,t)$ is contained in the array $\mathbf{U}(t)$. In general, any statement about the solution of the PDE is equivalent to a statement about its B-spline coefficients in (A1). POST actually computes $\mathbf{U}(t)$ and uses (A1) to evaluate the solution $\mathbf{u}(t,x)$.

The mechanism used by POST to handle PDE-ODE coupling is to say that the ODE variables $\mathbf{v}(t)$ are coupled to the PDE variables $\mathbf{u}(t,x)$ through the values of the B-spline coefficients $\mathbf{U}(t)$ of $\mathbf{u}(t,x)$, see (A1), and their partial derivatives with respect to t, $\mathbf{U}_t$. The PDE is assumed to have the form

$$\frac{\partial}{\partial x}\mathbf{a}(t,x,\mathbf{u},\mathbf{u}_x,\mathbf{u}_t,\mathbf{u}_{xt},\mathbf{v},\mathbf{v}_t)=\mathbf{f}(t,x,\mathbf{u},\mathbf{u}_x,\mathbf{u}_t,\mathbf{u}_{xt},\mathbf{v},\mathbf{v}_t)\ , \tag{A2}$$

where $\mathbf{a}$ and $\mathbf{f}$ are vector-valued functions of their arguments, for $L \le x \le R$. The boundary conditions are assumed to have the form

$$\begin{aligned}&\mathbf{b}_L(t,\mathbf{u}(t,L),\mathbf{u}_x(t,L),\mathbf{u}_t(t,L),\mathbf{u}_{xt}(t,L),\mathbf{v},\mathbf{v}_t)=\mathbf{0}\ ,\\ &\mathbf{b}_R(t,\mathbf{u}(t,R),\mathbf{u}_x(t,R),\mathbf{u}_t(t,R),\mathbf{u}_{xt}(t,R),\mathbf{v},\mathbf{v}_t)=\mathbf{0}\ ,\end{aligned} \tag{A3}$$

where $\mathbf{b}_L$ and $\mathbf{b}_R$ are vector-valued functions, of length n_u, of their arguments. The ODE's determining the ODE variables $\mathbf{v}$ are assumed to have the form

$$\mathbf{d}(t,\mathbf{U}(t),\mathbf{U}_t,\mathbf{v},\mathbf{v}_t)=\mathbf{0}\ , \tag{A4}$$

where $\mathbf{d}$ is a vector-valued function of its arguments. The length of $\mathbf{d}$ must be the number of ODE variables, n_v, that is, the length of the vector $\mathbf{v}$.

Consider the example of a linear Fredholm integro-differential equation of the form

$$u_t=u_{xx}+\int_0^1 c(x,y)u(y,t)dy \quad \text{for } x\in(0,1)\ , \tag{A5}$$

where $c(x,y)$ is some given kernel. We now recast (A5) in the form of (A2)–(A4) by introducing ODE variables $v_1(t),\ldots,v_N(t)$, where N is the number of basis functions to be used in the spatial discretization of the problem. Let

$$\mathbf{d}=\mathbf{v}-\mathbf{U}=\mathbf{0}\ .$$

Then $\mathbf{v}\equiv\mathbf{U}(t)$ and we can functionally couple u back into the PDE (A5) via $\mathbf{v}$. To see this, note that from (1) we have

$$\int_0^1 c(x,y)u(y,t)dy=\sum_i U_i\int_0^1 c(x,y)B_i(y)dy\ .$$

If we let $c_i(x)\equiv\int_0^1 c(x,y)B_i(y)dy$, this lets us rewrite (A5) as

$$u_t=u_{xx}+\sum_{i=1}^{N} v_i(t)c_i(x)\ ,$$

which has the desired form (A2)–(A4).

Our integral operators are linear for both Fredholm and Volterra equations. We used a standard k-point Gaussian quadrature rule to evaluate the integrals, where k is the B-spline order used.

The cost of evaluating the integral operators at each instant of time is $O(n_v^2)$. However, the run time of POST is dominated by the time to solve the resultant linear systems of equations, which is $O(n_v^3)$. Significant reductions in run time can be obtained, on machines such as the Cray, by vectorizing both the integration rules and the matrix solution methods. As a result the observed run time behaved more like $O(n_v^2)$ and the cost was quite modest. We note that quasi-Newton methods can be effective in cases where the kernel $c(x,y)$ is strongly peaked about $x=y$, resulting in a further reduction in the complexity of the matrix solution methods.

[1]A. A. Grinberg and S. Luryi, Phys. Rev. Lett. **65**, 1251 (1990).
[2]I. S. Gradshteyn and I. M. Ryzhik, in *Table of Integrals, Series and Products: Corrected and Enlarged Edition,* edited by A. Jeffrey (Academic, New York, 1980), p. 1075.
[3]A. A. Grinberg and S. Luryi, Phys. Rev. B **43**, 1812 (1991).
[4]A. A. Grinberg and S. Luryi, Phys. Rev. B **42**, 1705 (1990).
[5]F. Venturi, E. Sangiorgi, S. Luryi, P. Poli, L. Rota, and C. Jacoboni, IEEE Trans. Electron Devices **38**, 611 (1991).
[6]E. M. Conwell, *High Field Transport in Semiconductors* (Academic, New York, 1967).
[7]L. D. Landau, Zh. Eksp. Teor. Fiz. **7**, 199 (1937).
[8]N. L. Schryer, Bell Laboratories Computing Science Technical Report No. 115, 1984 (unpublished).
[9]U. Ravaioli, in *Monte Carlo Device Simulation: Full Band and Beyond,* edited by Karl Hes (Kluwer Academic, Dordrecht, in press), Chap. 9, p. 267.
[10]F. Venturi, R. K. Smith, E. Sangiorgi, M. R. Pinto, and B. Riccò, IEEE Trans. Comp. Aided Design **CAD-8**, 360 (1989).
[11]P. Lugli, and D. K. Ferry, Physica B **117**, 594 (1985); K. Sadra, C. M. Maziar, and B. G. Streetman, IEE Proc. **135I**, 119 (1988).
[12]W. Fawcett, A. D. Boardman, and S. Swain, J. Phys. Chem. Solids **31**, 1963 (1970); M. A. Littlejohn, J. R. Hauser, and T. H. Glisson, J. Appl. Phys. **48**, 4587 (1977).
[13]C. deBoor, *A Practical Guide to Splines,* Applied Mathematical Sciences Vol. 27 (Springer, New York, 1978).